SLAC-PUB-8190
July 1999

Beam Profile Measurement at 30 GeV Using Optical Transition Radiation

P. Catravas *et al.*

Presented at IEEE Particle Accelerator Conference (PAC 99),
3/29/99ã4/2/99, New York, NY, USA

Stanford Linear Accelerator Center, Stanford University, Stanford, CA 94309

Work supported by Department of Energy contract DE AC03 76SF00515.

BEAM PROFILE MEASUREMENT AT 30 GEV USING OPTICAL TRANSITION RADIATION*

P. Catravas,† W. P. Leemans, E. Esarey and M. Zolotorev, LBNL, Berkeley, CA 94720
D. Whittum, R. Iverson, M. Hogan, and D. Walz, SLAC, Stanford, CA 94309

Abstract

We present results of measurements of spot size and angular divergence of a 30 GeV electron beam though use of optical transition radiation (OTR). The OTR near field pattern and far field distribution are measured as a function of beam spot size and divergence at wavelengths of 441, 532, and 800 nm, for both the single and double foil configurations. Electron beam spot sizes of 50μm rms have been resolved, demonstrating the utility of OTR for measurement of small beam spot sizes of high energy (30 GeV) electron beams. Two-foil interference was clearly observed and utilized to extract electron beam angular divergences of $\sim 100\mu$rad.

1 INTRODUCTION

The theory of transition radiation was first introduced by Frank and Ginzburg in the first half of the century [1] and was further developed in the late 1950's by Garibyan [2] and others. Transition radiation has been widely used in high energy physics for particle identification, as well as for diagnosis in accelerator research. A comprehensive body of experimental work in the area of accelerator beam diagnosis currently covers a large range of beam energies, from 10's to 100's of MeV for visible transition radiation [3, 4], while most work at multi-GeV energies shifts to the X-ray portion of the spectrum [5]. Only recently, work has been performed in the visible wavelengths at energies up to 3.2 GeV and detailed discussions of the spatial resolution of OTR have been presented (see for example [6]-[9]).

In this paper, results are presented of the diagnostic implementation of optical transition radiation for a 30 GeV electron beam. Spot sizes as low as 50 μm rms have been resolved using radiation at 532 nm and beam divergences on the order of $\sim 100\mu$rad have been obtained using the double foil configuration. Spot size resolution is consistent with what is expected from the collection angle of the optical imaging system.

2 CONCEPT

Diagnostic spatial resolution, d, is determined by diffraction: $d \sim \lambda/\theta$, where λ is the radiation wavelength and θ is the collection angle. Typically, radiation from highly relativistic electrons is concentrated in a cone of width $1/\gamma$, which makes it difficult to measure spots of high γ beams with sufficient spatial resolution. In contrast, while the angular distribution of OTR photons does peak at the angle $1/\gamma$, the intensity falloff outside the $1/\gamma$ cone is much slower than, for example, that of synchrotron radiation. The fraction of energy inside the $1/\gamma$ cone drops with increasing energy, giving OTR utility for beam diagnosis at ultra-relativistic energies. The OTR angular distribution from a single electron for a metal foil is

$$\frac{d^2W_1(\theta)}{d\omega d\Omega} \sim \frac{\theta^2}{(\gamma^{-2}+\theta^2)^2} \approx \frac{1}{\theta^2}, \quad \frac{1}{\gamma} \ll \theta \ll 1, \qquad (1)$$

which is valid for both backward and forward OTR if the photon energy is smaller than ~ 10 eV, the typical energy corresponding to the plasma frequency of metallic foils.

While beam divergence can in principle be obtained from the far field pattern of a single foil, the two foil interferometer, as developed by L. Wartski [3], is often preferred as it provides increased sensitivity to beam divergence[4]. Furthermore, the two-foil interferometer provides control over the angular resolution, unlike the single foil configuration, for which the resolution is fixed at each beam energy. In the two-foil interferometer, forward radiation from an upstream foil combines with backward radiation from a second foil located a distance L downstream, yielding an addition of phases of $1-\exp\left[-j\pi(\gamma^{-2}+\theta^2)L/\lambda\right]$. The interference term depends on the formation length, $L_f = (\lambda/\pi)(\gamma^{-2}+\theta^2)^{-1}$ (written for vacuum, $\gamma \gg 1$ and $\theta \ll 1$) [2, 3]. The angular intensity distribution [3] for the two foil interferometer for large angles ($\theta \gg 1/\gamma$) becomes

$$\frac{d^2W_2(\theta)}{d\omega d\Omega} \sim \frac{1}{\theta^2}\sin^2\left(\frac{L}{2L_f}\right), \qquad (2)$$

where $L_f \simeq \lambda/(\pi\theta^2)$. After convolution of the two-foil interference pattern for a single electron with a Gaussian electron beam distribution of angular width σ_θ, the angular intensity distribution can be written,

$$\frac{d^2W_2(\theta,\sigma_\theta)}{d\omega d\Omega} = 2\frac{d^2W_1(\theta)}{d\omega d\Omega}G, \qquad (3)$$

where

$$G = \left[1-\exp\left(-2\pi^2L^2\sigma_\theta^2\theta^2/\lambda^2\right)\cos\left(\pi L\theta^2/\lambda\right)\right]. \quad (4)$$

* Work supported by the U.S. Department of Energy under contract No. DE-AC-03-76SF0098.

† Email: PECatravas@lbl.gov

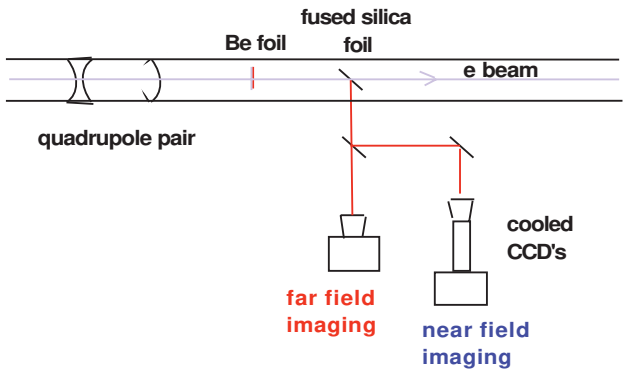

Figure 1: Experimental setup.

3 EXPERIMENTAL SETUP

The experiments were performed in the FFTB beamline at SLAC. The experimental setup is shown in Fig. 1. An aluminum coated fused silica substrate (150μm thick) was located 0.56 m downstream from a retractable, 25 μm thick Beryllium foil. The backward reflected OTR was split by a pellicle beamsplitter between two cooled CCD cameras, 16 bit and 12 bit, providing simultaneous images of the near and far field, respectively. The near field resolution was determined using a resolution target and was 10 μm or better. This is consistent with the collection angle of 0.1 rad. The available field of view was approximately 3 mm. Far field resolution was set at $6/\gamma$ radians per pixel. For this experimental run, the beam energy was 28.5 GeV, and single microbunches with about 1.5x10^{10} particles with normalized vertical and horizontal emittances of 0.47x10^{-5} m-rad and 6.5x10^{-5} m-rad were used.

4 RESULTS

4.1 *Spot size measurement*

Results from near field imaging of the OTR from a single foil (fused silica inserted, Be removed from the beam path) are shown in Fig. 2. Quad scans were performed in the vertical and horizontal axes, and OTR images were recorded as the scans passed through and beyond a waist at the foil location. The series of five images shown in Fig. 2 are near field images recorded by the cooled CCD during the horizontal and vertical quad scans. The accompanying plots contain the complete set of extracted rms beam sizes as a function of quadrupole strength. Beam spot sizes of 50μm were resolved in both axes in a single shot measurement.

Beam spot size resolution and photon yield were compared with and without the addition of the second foil (Be at 0.56 m upstream). No difference was observed in either the measured spot size or the number of collected photons. This observation is consistent with the depth of focus of the near field imaging of our setup, which was small compared with the foil separation; only the photons from one foil were well imaged onto the CCD chip.

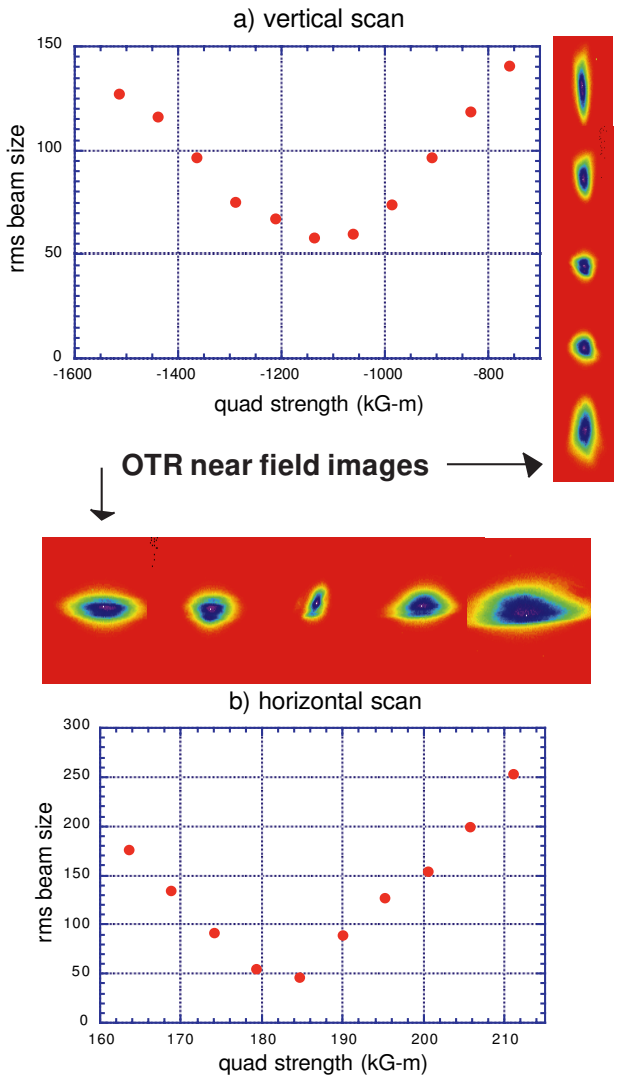

Figure 2: Spot size measured with OTR and near field images for vertical and horizontal quadrupole scans.

4.2 *Angular divergence measurement: two-foil interferometry*

Interference patterns were recorded from the two-foil interferometer at a variety of wavelengths: 441, 532, 632, 800, and 1064 nm. The appearance of the intensity maxima is well described by Eq. (2) both as a function of angle and as a function of wavelength. In Fig. 3, two-foil interference patterns centered at 441 and 800 nm display the expected increase in peak separation with wavelength. At 28.5 GeV, $\lambda = 532$ nm, and foil separation $L \sim 0.6$ m, the first interference maximum is expected and observed at angle of $50/\gamma$. Note that if one wishes to set the first interference maximum near $1/\gamma$, then the required foil separation length, $\lambda\gamma^2/2\pi$, is on the order of a km, which is comparable to the total length of the SLAC linac.

Foil separation L is chosen only according to the range of divergence one wishes to diagnose. From Eqs. (3)-(4), one can see that the angular resolution (minimum resolv-

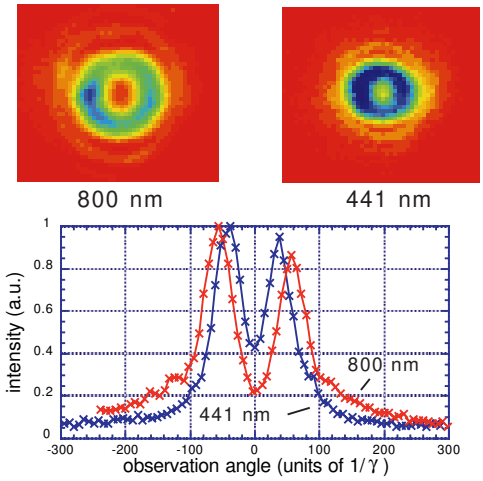

Figure 3: Comparison of two-foil interference at 441 and 800 nm shows expected wavelength dependence.

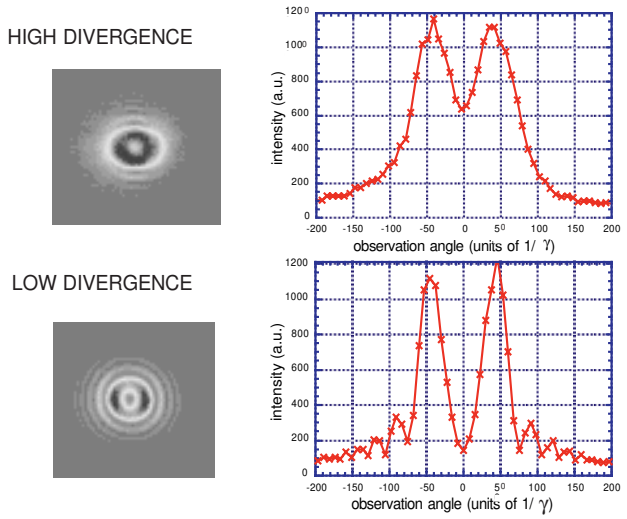

Figure 4: Two foil interference during a quadrupole scan evolves from no modulation to full modulation, indicating that realistic beam parameters can be diagnosed.

able divergence) is $\sigma_{res} = d/L$. For the far field imaging, the effective collection angle was considerably smaller than for the near field imaging, and was approximately 3 mrad, corresponding to $d = 30$ μm. Chosing a foil separation L of 0.6 m gives an angular resolution of 50 μ rad. Note also that from the practical point of view, the spatial and angular resolution become independent of the beam energy.

Sensitivity of the far field pattern to changes in beam divergence was studied by performing a quadrupole scan to vary the divergence. The resulting profiles (Fig. 4) shifted from nearly full modulation to no modulation as the divergence was increased. Futhermore, in Fig. 4(a), an absence of modulation in the horizontal axis was observed while clear modulation was present in the vertical axis. This is consistent with known difference in vertical and horizontal emittance at the FFTB. Divergences of $\sigma_\theta \sim 100$ μrad were extracted from the data using Eq. 3 and 4.

The descibed techniques were developed in support of the E157 experiment [10] at the FFTB at SLAC, which will study the interaction of the 30 GeV beam with a long plasma column. In effect, the OTR foils have been designed into the setup in such a way that they serve a double purpose. One of the foils will separate a plasma volume from an ultra-high vacuum section of beampipe; the other doubles as an Excimer incoupler. Viewing OTR in this compact fashion will provide non-destructive diagnostic information for the E157 experiment as close as possible to the interaction region. OTR will be collected both at the oven entrance and exit to determine beam parameters directly at the experiment entrance as well as after interaction with the plasma. Because this interaction is expected to produce large changes in the beam spot size and divergence which are time varying, streaking the OTR at the oven exit is planned.

5 CONCLUSIONS

Measurements of transition radiation in the visible wavelengths have been performed at nominally 30 GeV at the FFTB beamline at SLAC. Spot sizes on the order of 50μm have been measured with OTR at this energy and wavelength. Beam divergences of approximately 100 μrad have been calibrated with a two-foil interferometer.

6 ACKNOWLEDGMENTS

The authors thank Leon Archambault, Scott DiMaggio and Jim Dougherty for their technical assistance.

7 REFERENCES

[1] V.L. Ginzburg and I.M.Frank, Sov. Phys. JETP 16, 15 (1946).

[2] G.M. Garibyan, Sov. Phys. JETP 6, 1079 (1958); *Ibid.*, Sov. Phys. JETP 10, 372 (1960).

[3] L. Wartski et al., J. Appl. Phys., 46, 3644-3653 (1975).

[4] D.W. Rule, Nucl. Inst. & Meth., B24/25, 901 (1987); *Ibid.* et al., Nucl. Instr. & Meth. A 296, 739 (1990); A.H. Lumpkin et al., Nucl. Instr. & Meth. A, 296, 150 (1990); R.B. Fiorito et al.,1991 PAC Proc., 2, 1204, (1991); A.H. Lumpkin (Ed.), Proc. 1996 Beam Instrum. Workshop, AIP Conf. Proc. 390 (1997); W.P. Leemans et al., Phys. Rev. Lett. 77, 4182 (1996); A.H. Lumpkin, Nucl. Instr. & Meth. A 393, 170 (1997).

[5] L.C.L. Yuan et al., Phys. Rev. Lett., 25, 1513-1515 (1970).

[6] P. Piot et al., Proc. 1996 Beam Instrumentation Workshop, AIP Conf. Proc. 390, 298 (1997).

[7] X. Artru et al., Nucl. Instr. & Meth. A 410, 148-158 (1998).

[8] D.W. Rule, R.B. Fiorito, AIP Conf. Proc. 229, 315 (1991).

[9] M. Castellano and V. A. Verzilov, Phys. Rev. Special Topics, 1, 062801-1 (1998).

[10] R. Assman et al., these Proceedings, FRA113.

[11] P. Muggli et al., these Proceedings, FRA115; S. DiMaggio et al., these Proceedings, FRA138